

Morphological evidence for marine ice stream shutdown, central Barents Sea

Bartosz Kurjanski^{a,*}, Brice R. Rea^a, Matteo Spagnolo^a, Monica Winsborrow^b, David G. Cornwell^a, Karin Andreassen^b, John Howell^a

^a School of Geosciences, University of Aberdeen, AB24 3UE, Scotland, UK

^b Centre for Arctic Gas Hydrate, Environment and Climate (CAGE), The Arctic University of Norway, N-9037 Tromsø, Norway

ARTICLE INFO

Editor: Michele Rebecco

ABSTRACT

Marine-based ice streams are responsible for a significant proportion of the ice mass loss from the present-day Greenland Ice Sheet, East Antarctic Ice Sheet (EAIS) and West Antarctic Ice Sheet (WAIS) but the processes controlling their initiation, evolution and shutdown remain elusive, hindering our understanding of how existing ice masses will respond to predicted future warming. The exposed beds of palaeo-ice streams offer a unique opportunity to study subglacial processes, which are largely inaccessible in contemporary settings. We use high resolution multibeam swath bathymetry data from the Barents Sea to map the geomorphology of a palaeo-ice stream bed, located in Olgastretet (Olga Trough), approximately 75 km southeast of Kong Karls Land and 200 km east of central Svalbard. This reveals evidence for shut down of a marine-based ice stream, followed by a phase of passive retreat or lift-off of the ice stream facilitating preservation of crevasse-squeeze ridges (CSRs). Subsequently, active retreat of the ice margin was re-established and is marked by recessional moraine ridges located upstream of the CSRs. Previously, CSRs have been mainly associated with surging land-terminating ice margins, however our work adds to recent observations of CSRs on the beds of marine-based ice streams, implying that they may be more common than previously thought. It also indicates that marine-based ice streams may switch on- and off in a surge-like manner which has important implications for our understanding of ice stream life cycles and the modelling of ice sheets.

1. Introduction

It is estimated that up to 50% of the mass loss from the Greenland Ice Sheet (Enderlin et al., 2014) and 90% mass loss from the Antarctica Ice Sheet (Bennett, 2003) is accomplished by the flow of ice to the ocean, via marine terminating ice-streams. These arteries of ice move with velocities up to 1500 ma^{-1} (Bennett, 2003; Thomas et al., 2013), at least an order of magnitude higher than surrounding inter-ice stream areas. Observation from contemporary ice streams show that their velocity may change rapidly and by orders of magnitude (Clarke, 1987; Engelhardt and Kamb, 2013; Joughin et al., 2002; Rignot et al., 2002), which has implications for both the mass balance and dynamics of ice sheets. Understanding these variations is crucial not only to understand contemporary ice-stream dynamics but also how they will respond to future climate and sea level changes. Processes occurring subglacially are considered to have fundamental control on ice stream behaviour (Bingham et al., 2017). Understandably accessing and studying the subglacial domain of a contemporary ice stream is extremely challenging. Therefore, investigating exposed beds and bedforms of palaeo-ice

streams offers a unique opportunity to better our understanding of mechanisms governing ice stream dynamics and evolution. One of the best areas to conduct such studies is the Barents Sea where ice streams are believed to have played a major role during the deglaciation of the Barents Sea ice sheet (BSIS) (Fig. 1) following the Last Glacial Maximum (Andreassen et al., 2014b; Bjarnadóttir, 2016; Bjarnadóttir et al., 2014; Ingólfsson and Landvik, 2013; Nielsen and Rasmussen, 2018; Patton et al., 2017; Siegert and Dowdeswell, 1996). The BSIS has similar characteristics to, and can serve as an ideal analogue for, the present-day West Antarctic Ice Sheet i.e. they are comparable in size, are/were marine terminating and grounded largely below sea level, on the continental shelf.

The geomorphology of a palaeo ice stream bed, located in the Olgastretet (Olga Trough) (Fig. 1), approximately 75 km southeast of Kong Karls Land and 200 km east of central Svalbard, is mapped in this paper and used to reconstruct the ice stream margin geometry, ice flow directions and ice stream dynamics (Fig. 2). Recently-acquired high spatial resolution bathymetric data enabled mapping at unprecedented detail, which in turn allowed us to recognise a suite of landform

* Corresponding author.

E-mail address: bkurjanski@abdn.ac.uk (B. Kurjanski).

<https://doi.org/10.1016/j.margeo.2019.05.001>

Received 26 January 2019; Received in revised form 25 April 2019; Accepted 1 May 2019

Available online 02 May 2019

0025-3227/ © 2019 The Authors. Published by Elsevier B.V. This is an open access article under the CC BY license (<http://creativecommons.org/licenses/by/4.0/>).

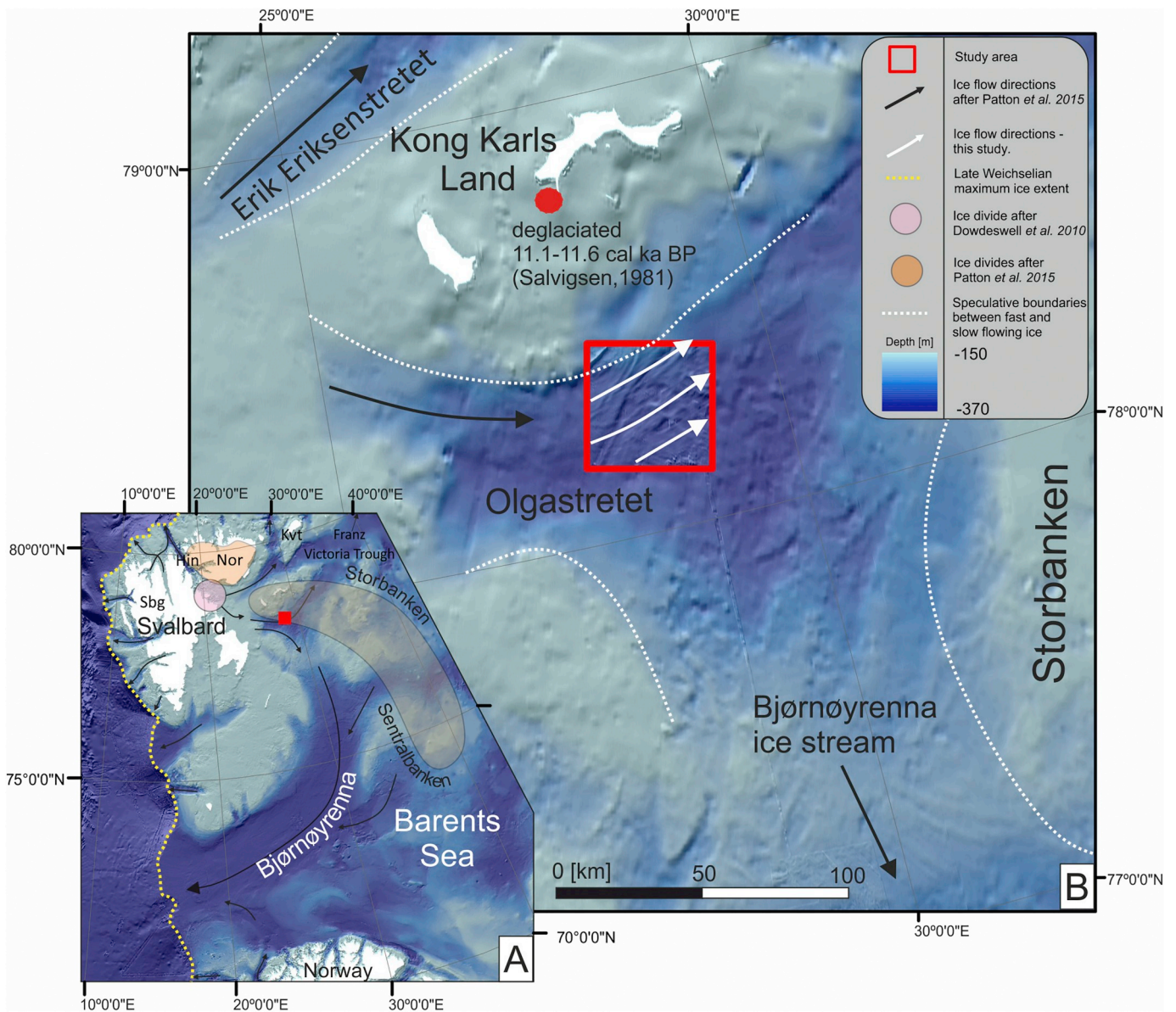


Fig. 1. (A). Location map of the western Barents Sea. Black arrows indicate palaeo-ice flow directions from [Patton et al. \(2015\)](#), linked to the Late Weichselian ice flow. The red square indicates the location of the study area. (B) Study area in upper Bjørnøyrenna, northwestern Barents Sea. The red box indicates the extent of the multibeam swath bathymetry dataset used in this study. White arrows indicate palaeo-ice flow direction in Olga Trough identified in this study. Kvt - Kvitøya, Nor - Nordaustlandet, Sbg - Spitsbergen, Hin - Hinlopenstret. (For interpretation of the references to color in this figure legend, the reader is referred to the web version of this article.)

assemblages that provide evidence for shutdown followed by later re-activation of a marine ice stream, in a deep-water (~250–450 m) setting (Fig. 2). The landform assemblage has striking similarity to the terrestrial surging glacier landsystem (e.g. [Benediktsson, 2009](#); [Evans and Rea, 1999](#); [Ingólfsson et al., 2016](#); [Ottesen et al., 2017](#); [Streuff et al., 2015](#)).

1.1. Study area

The large-scale bathymetry of the epicontinental Barents Sea is characterised by shallow banks (water depths ~100–200 m) and cross-shelf troughs (water depths ~300–500 m), extending to the shelf edge (Fig. 1). The largest Barents Sea trough, Bjørnøyrenna (Bear Island Trough), extends for over 700 km, and is over 200 km at its widest. Large depocentres (trough mouth fans) have developed on the continental slope, immediately beyond the cross-shelf troughs, documenting significant glacial erosion of the Barents Sea shelf (e.g.

[Batchelor and Dowdeswell, 2014](#); [Laberg and Vorren 1996](#); [Torbjørn Dahlgren et al., 2005](#)). The thickness of glacial sediments on the shelf is variable, but rarely exceeds 100 m ([Solheim and Kristoffersen, 1984](#); [Elverhøi and Solheim, 1983](#); [Andreassen et al., 2008](#)).

Based on clay mineral and ice-rafted debris records from boreholes, grounded ice is first suggested to have glaciated parts of the Barents Sea in the Pliocene (3.6 Ma), and continued to be periodically present in the basin through the Pleistocene, with multiple cycles of ice advance and retreat ([Knies et al., 2009](#)). Around 1.5–1 Ma, northern hemisphere glaciations intensified, and the general view is that from this time ice sheets repeatedly covered the Barents Sea all the way to the continental shelf. At its maximal extent, the BSIS and the Fennoscandian Ice Sheet (FIS) merged. On coalescence, major trough mouth fans began to form, via the supply of sediments to the shelf edge by ice streams draining the interior of the BSIS. Deglaciation of the region started after the global Last Glacial Maximum (LGM) 21.5–18.1 cal. ka BP (e.g. [Rasmussen et al., 2007](#); [Rüther et al., 2011](#)). Between 17 and 14 cal. ka BP the BSIS

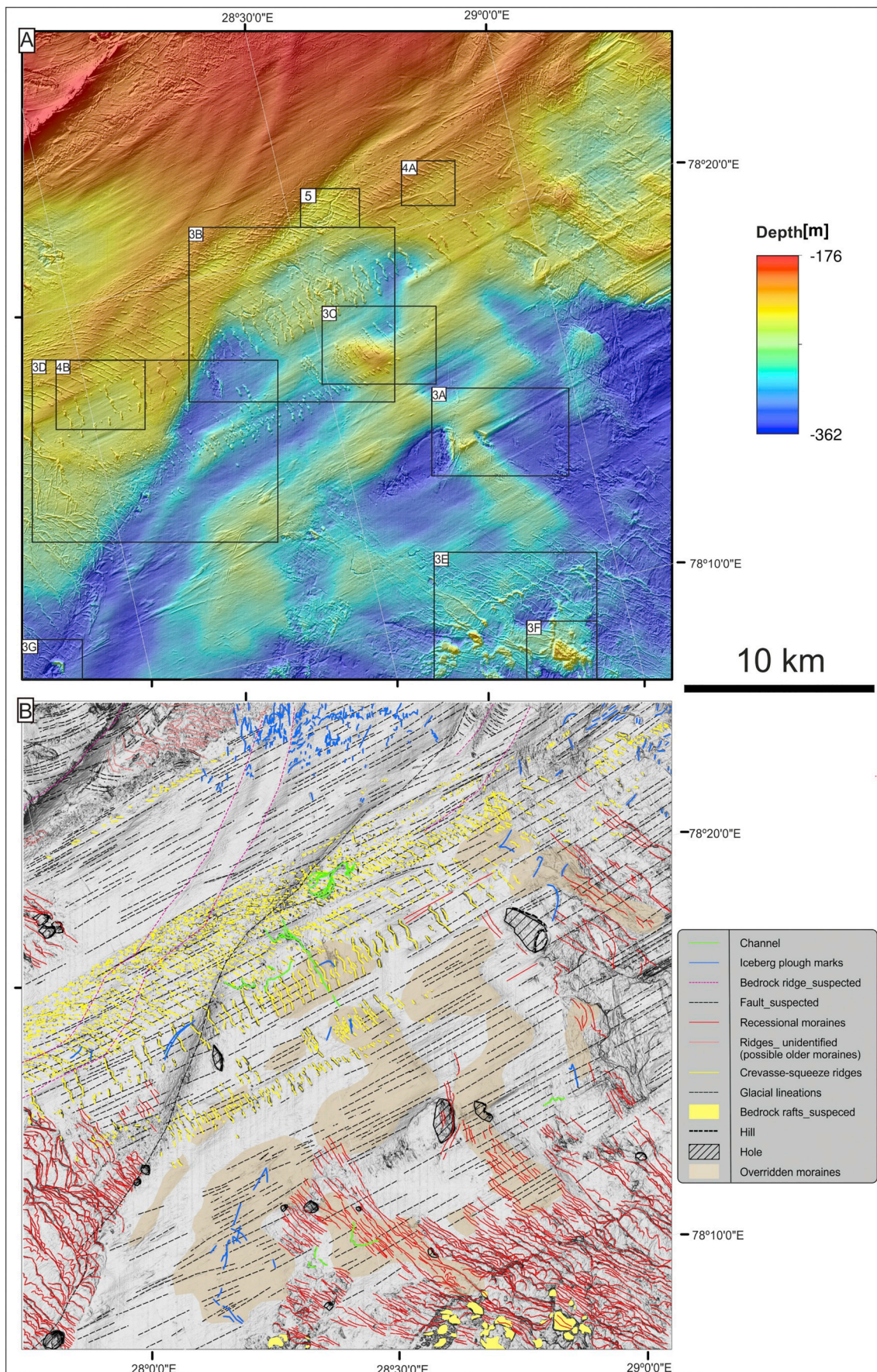


Fig. 2. A: Seabed geomorphology of the study area courtesy of MAREANO (www.mareano.no). Black rectangles refer to areas shown in Figs. 4 and 5 B: mapped distribution of landforms in the study area.

is thought to have separated from the FIS and by 11.2 cal. ka BP most of the Barents Sea was ice-free (e.g. Polyak et al., 1995; Salvigsen, 1981; Landvik et al., 1992; Hughes et al., 2016; Winsborrow et al., 2010). According to a compilation of available chronological data, the area of interest in this study (Olgastretet) deglaciated between 16 and 11.7 cal. ka BP (Hogan et al., 2010; Hughes et al., 2016). The study area is particularly interesting when the history of the BSIS is considered. Olgastretet was located close to the inferred major ice accumulation centre during the LGM (Esteves et al., 2017; Ingólfsson and Landvik, 2013; Newton and Huuse, 2017; Nielsen and Rasmussen, 2018). During deglaciation, Olgastretet was at the boundary between the SSE-draining Bjørnøyrenna ice stream and a NE-draining ice stream flowing towards the Kvitøja Trough and Franz-Victoria Trough (Dowdeswell et al., 2010; Nielsen and Rasmussen, 2018; Patton et al., 2016). Hogan et al. (2010) and Dowdeswell et al. (2010) demonstrated, by mapping glacial landforms on the seabed, that later in the deglaciation, an E-flowing ice stream located in Olgastretet flowed NE around Kong Karls Land draining the Svalbard area with the ice centre located in Hinlopenstret, between Spitsbergen and Nordaustlandet. Their interpretations of the location of the ice centre does not fully match with the landform assemblage later mapped in the upper part of the Bjørnøyrenna (Andreassen et al., 2014a, 2014b), testifying to the complex history of ice divide migration during the deglaciation of the BSIS. Further attempts to reconstruct the glacial history of this particular sector of the BSIS in greater detail were hampered by a paucity of high-resolution geophysical data (bathymetry and seismic) and a limited number of widely-spaced age control points (Dowdeswell et al., 2016; Hogan et al., 2010)

2. Methodology

High resolution bathymetry of Olgastretet acquired in 2015 is now available via MAREANO (www.mareano.no). The dataset covers an area of 1008 km², and was gridded to 10 m horizontal resolution. Analysis of the multibeam bathymetry was carried out in ArcGIS and glacial landforms were mapped and interpreted based on their expression on the bathymetric digital terrain model, overlain with 50% transparent hillshade rasters. The Line Density Tool in ArcGIS was used to measure, and map, the density of linear features (km/km²). The search radius was set to 500 m and the output raster cell size was set to 50 m. The regional bathymetry was provided by EMODnet Bathymetry Consortium, 2016 (<http://www.emodnet-bathymetry.eu>) at a resolution of 0.125 arcminute, which translates to ~300 m at the latitude of the central Barents Sea.

3. Landform assemblages

3.1. Lineations and moulded subglacial landforms

Two major types of subglacially-moulded landforms are identified in the study area (Fig. 2). The first type consists of elongated ridges and/or grooves that are consistently parallel to subparallel, 70–460 m wide, 220–8800 m long (mean 1853 m) and 0.4–2.2 m high (Fig. 3A). They are oriented WSW–ENE and are present across the entire study area, with the exception of the SW and SE corners. The elongation ratios of the grooves / ridges (5:1–46:1, mean 7.4:1), relief, width and length fit well with published metrics of mega scale glacial lineations (MSGL) (Spagnolo et al., 2014; Ely et al., 2016) and we interpret them as such. Their spacing (80–900 m) is also consistent with that observed in other datasets worldwide (Spagnolo et al., 2017). MSGLs were first identified in the landform record and interpreted to form subglacially beneath streaming ice (Clark, 1993; Clark and Stokes, 2001). This interpretation has been subsequently confirmed by observations of MSGLs forming beneath contemporary fast-flowing glacial systems (King et al., 2009; Bingham et al., 2017; Ottesen et al., 2017). The presence of MSGLs indicates that the study area was once occupied by an ice stream,

flowing along a WSW–ENE axis.

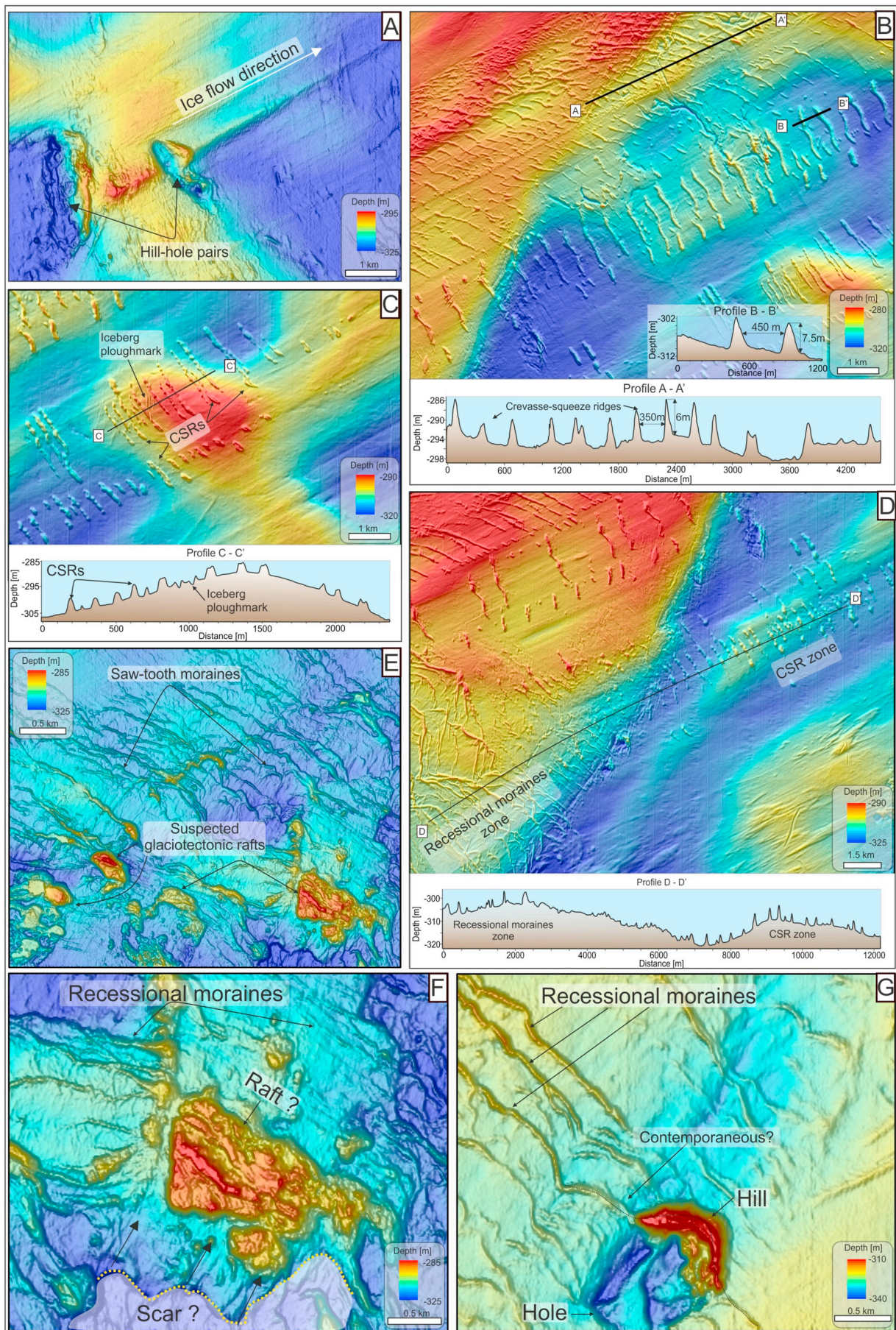
A second group of streamlined landforms is located in the centre of the study area (Fig. 2B). This region comprises low relief and irregular mounds with superimposed MSGLs. The mounds are 8–25 m high, 10 km long and 11 km wide (length and width measured parallel and perpendicular, respectively, to the inferred ice stream flow). Their elongation ratio (0.28:1–2.16:1), dimensions and irregular shape make it difficult to assign these mounds to any “classic” subglacial landform (Ely et al., 2016). The streamlining of the mounds and the presence of superimposed MSGLs on their surface indicates that they predate ice streaming in the study area. They are interpreted as overridden moraines and/or grounding zone wedges (Ottesen et al., 2017) and were likely deposited during an earlier ice margin still-stand or re-advance.

3.2. Crevasse-squeeze ridges

In the central part of the study area is a prominent ridge complex comprised of multiple, angular segments trending between N055E° and S125E°, perpendicular to sub-parallel to the ice flow direction (Fig. 2). Individual segments are between 0.5 and 8 m (mean 3.2 m) high and 20–800 m (mean 188 m) long (measured from the long axis of the landform) and 30–270 m (mean 101 m) wide (Fig. 3B). Spacing and size distribution is variable with longer, higher and less densely-spaced ridges on the SE margin of the complex and shorter, lower and more densely-spaced segments on the NW margin. In the western part of the complex, the ridges appear to gradually change direction from SSE–NNW (ice-flow perpendicular) to WSW–ENE (ice-flow parallel) (Fig. 2 and Fig. 3). The ridges are superimposed on the MSGLs, postdating them (Fig. 3C). The scale and morphology of these features is typical of crevasse-squeeze ridges (CSRs) (Evans and Rea, 1999), which are formed by sediment in-filling basal crevasses. Bottom-up (basal) crevasse-squeezing occurs when basal water pressures are sufficiently high, and may be supplemented by extensional strain, to initiate hydrofracturing (Rea and Evans, 2011). Water-saturated subglacial sediments are squeezed into the crevasses during hydrofracturing or subsequently when the basal water pressure decreases, under the weight of overlying ice. CSRs are widely considered diagnostic of glacier surging and have been recognised in various settings worldwide (e.g. Benediktsson et al., 2009; Cofaigh et al., 2010; Evans and Rea, 1999; Ingólfsson et al., 2016). They have also been identified on palaeo-ice stream beds (Andreassen et al., 2014b; Bjarnadóttir et al., 2014; Evans et al., 2016) similar to that of this study area, and are suggested to be associated with the final stages of ice streaming and deglaciation, facilitating their preservation. The angular relationship between the individual segments of the CSRs retaining the shape of a conjugate fracture system (Fig. 4), lack of lateral continuity of ridges, and their offset in the direction parallel to the flow (Fig. 4A) together with discrete, ice stream flow-parallel units (Fig. 4), rule out an alternative interpretation for these ridges as De Geer moraines. Moreover, the preservation of underlying MSGLs would not have been possible if the ridges were in fact De Geer moraines as these are formed by the bulldozing of sediments during annual ice re-advances that would have destroyed the MSGLs, as most likely occurred for the moraines discussed in Section 3.4.

3.3. Subglacial channels

In seven locations in the centre of the study area, anabranching, sinuous or linear, negative relief landforms are visible (Fig. 5). They are 1100–5500 m long, 35–130 m wide (individual incisions) and up to 6 m deep. They are almost-exclusively situated on the seabed within the area where CSRs are preserved. Their orientation varies between individual features and does not seem to correspond to the overall ice flow direction (Fig. 2). Collectively, their shape resembles a channel network (Dowdeswell et al., 2016; Dowdeswell and Bamber, 2007; Newton and Huuse, 2017; Simkins et al., 2018) or the plough marks of a multi-keel iceberg. However, they lack the elevated banks typical of



(caption on next page)

Fig. 3. Detailed seabed morphology of selected glacial landforms within the study area. For location see Fig. 2. A: Subglacial lineations (MSGLs) indicate ice flow direction to the NE. B: CSRs identified in the central part of the study area. C: CSRs superimposed on subglacial lineations. Note an iceberg ploughmark cutting some of the CSRs. D: CSRs and recessional moraines. The preservation of CSRs in the NE part of the area is suggested to reflect ice margin lift-off or passive retreat, whilst recessional moraine ridges indicate the area where the ice margin was retreating actively. E: Recessional moraines documenting active ice margin retreat. Note the festoon-like shape of some of the ridges. F: Possible subglacial bedrock raft. G: Hill-hole pair surrounded by recessional moraines. In some cases recessional moraines are continuing into hills implying contemporaneous formation of both landforms. H: Suspected subglacial meltwater channel. Note its anastomosing, sinuous form and lack of elevated flanks allows channels to be distinguished from iceberg ploughmarks.

iceberg plough marks; their smooth sinuous form and the fact that grooves are not parallel indicates that they were most likely formed by channelized flow of water. They are therefore interpreted as channels formed by erosion in a subglacial drainage network. The CSRs appear to be cross-cut by the channel in places, whilst in other locations they appear to be preserved on the seabed and within the channel (Fig. 5). We suggest two possible interpretations: 1) The channel postdates CSRs formation and meltwater erosion was insufficient to remove all of the CSR material or preferentially melted out the ice above the CSRs; or 2) CSRs postdate channel formation and the remaining deposits within the channel are evidence of the release from ice and collapse of the CSR material into over-deepened parts of the channel.

3.4. Linear and curvilinear saw-tooth moraine ridges

Curvilinear and festoon-like ridges (Fig. 3D & E) cover the SW and S part of the study area. They are often amalgamated and branching, between 100 and 6700 m long, 100–800 m wide and up to 15 m high. Their morphology is different from that of the CSRs identified in the central sector (Fig. 3D). No MSGLs are observed where the ridges are present (Fig. 6A & C). The ridges are more continuous and less angular than the CSRs. They are often interconnected, with individual centres of a ridge segment curving down ice flow, and the sides pointing up ice. These ridges are interpreted as recessional moraines/saw-tooth moraines (Matthews et al., 1979) and were partially described from this exact area by Hogan et al. (2010). They are interpreted to record the active retreat of a back-stepping ice margin that is punctuated by periodic advances, rather than passive retreat. A lack of preserved, underlying MSGLs indicates reworking of the seabed by the oscillations of the ice margin. This implies that these moraines postdate ice streaming in the study area.

3.5. Glaciotectonic landforms

3.5.1. Hill-hole Pairs

Fifteen oval seabed depressions rimmed by a sediment ridge on their NE side are identified in the study area (Fig. 2 & Fig. 3G). The depressions are 200–2800 m wide and 150–1300 m long. Their depth varies between 2 and 12 m. The hills have a corresponding width range, are 80–450 m long with heights of 4–35 m. Volumetrically, the depressions are 8–13% smaller than the ridges (which may be within measurement inaccuracy) and they locally co-exist with and/or disrupt other landforms, such as recessional moraines or MSGLs. We interpret these as hill-hole pairs, which are glaciotectonic landforms and typically form when sediment is excavated, transported and deposited, forming a hill. They are often found in association with recessional moraines (Aber et al., 1989; Rise et al., 2016). Their orientation implies that ice was flowing towards the NE, which is similar to the WSW-ENE flow identified from the MSGLs. The holes are clearly erosional and are incised into the underlying MSGLs.

3.5.2. Suspected bedrock rafts

A group of flat-topped, irregular or oval mounds (11–25 m high) are present in the SE corner of the study area (Fig. 3E & F). These mounds are 100–1200 m in diameter. Some 1500 m up-flow, an over deepening (18–22 m) with relatively sharp margins is clearly seen in the bathymetry. Part of the over deepening lies outside of the study area and therefore it is impossible to provide a direct measurement for its exact diameter. The shape of the visible margin of the depression and its depth appear to correspond to the location of the NE margin of the mound (Fig. 3F). Some of the mounds have associated tails indicating ice over-riding and ice flow to the NE. We interpret them as locally eroded bedrock rafts (Rüther et al., 2013 and 2016) but an alternative interpretation of local bedrock highs cannot be ruled out without additional subsurface data (i.e. seismic or wells). Buried glaciotectonic rafts have recently been located under the Bjørnøyrenna ice stream, suggesting that they are more common than previously thought

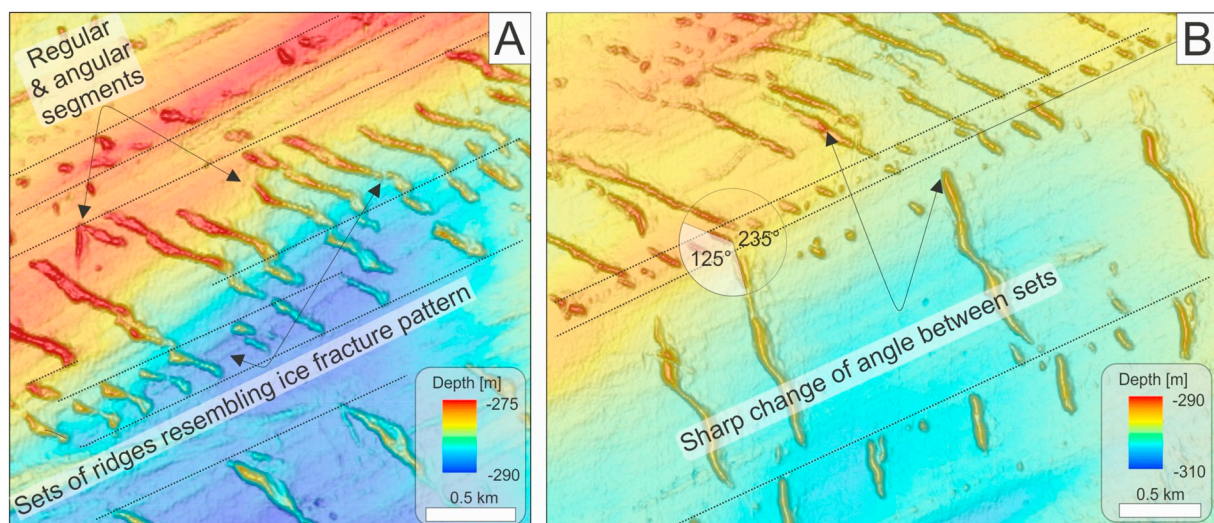


Fig. 4. Detail of CSRs. Note variable spacing between ridges, angular relationship between discrete sets and differences in lengths between individual segments. Unlike De Geer moraines the ridges do not follow a continuous trend, instead they terminate sharply and are offset with respect to another set of CSRs.

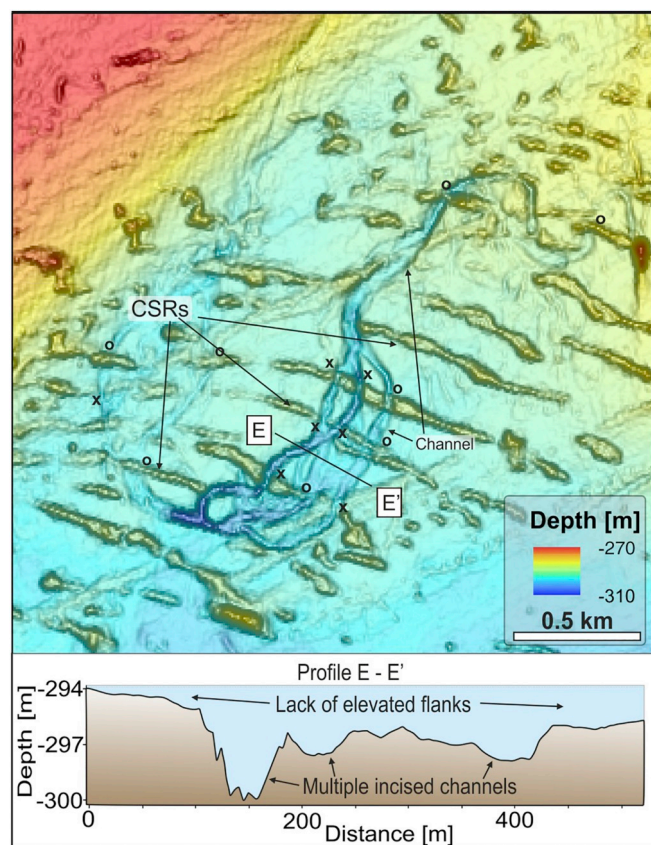


Fig. 5. Detailed image of a subglacial channel (3H). In places CSRs appear to be cross-cut by the channel (marked by X). In other locations CSRs seem to be preserved on the seabed and within the channel (marked by O). There are two possible interpretations: 1) The channel postdates CSRs formation and melt-water erosion was insufficient to remove all of the CSR material or preferentially melted out the ice above the CSRs, 2) CSRs postdate channel formation and the remaining deposits within the channel are evidence of the release from ice and collapse of the CSR material into over-deepened parts of the channel.

(Andreassen and Winsborrow, 2009; Bellwald et al., 2018).

3.6. Iceberg ploughmarks

Rare, linear and curvilinear grooves with elevated flanks are found in the study area (Fig. 2). Most of them are shallow, relatively short (60–2400 m long, mean 407 m) and located in the NE of the study area where the seabed is at least 60 m shallower than in the centre (Fig. 6D). In the deeper, central part of the study area only a few are present. They often cross-cut and displace CSR sediments and underlying MSGLs and are interpreted as iceberg ploughmarks. The rarity of iceberg ploughmarks in the study area indicates that, during deglaciation, either the area was covered by a mélange/sea ice capable of blocking or diverting drifting icebergs, or its water depth (~180–360 m) was greater than the draft of iceberg keels generated by a grounding line in shallower waters.

4. Discussion

4.1. Implications of formation and preservation of the crevasse squeeze ridges

The seminal description of CSRs came from land-terminating surging glaciers in Iceland by Sharp (1985), and they have subsequently been investigated in many other areas in contemporary and deglaciated

landscapes, for example: Svalbard (e.g. Boulton et al., 1996; Christoffersen et al., 2005; Flink et al., 2015; Streuff et al., 2015); Canada (Johnson, 1975; Clarke et al., 1984; Evans and Rea, 1999; Evans et al., 1999); and Iceland (e.g. Evans et al., 2009; Waller et al., 2008). The presence of CSRs in the landform record has been interpreted to indicate passive retreat of terrestrially-terminating glaciers and ice streams. This occurs when the ice stagnates and melts away in situ, facilitating landform preservation (Evans and Rea, 1999). As high resolution marine geophysical datasets become more widely available, CSRs have also been found on the seafloor proximal to terrestrial surging glaciers (Ottesen and Dowdeswell, 2006; Ottesen et al., 2008), motivating the development of a water-terminating surging glacier landsystem model (Ottesen et al., 2017). In such settings, preservation of CSRs can most easily be explained by ice margin stagnation followed by in situ melting leading to lift-off (flotation) of the ice from the seabed facilitating a passive retreat.

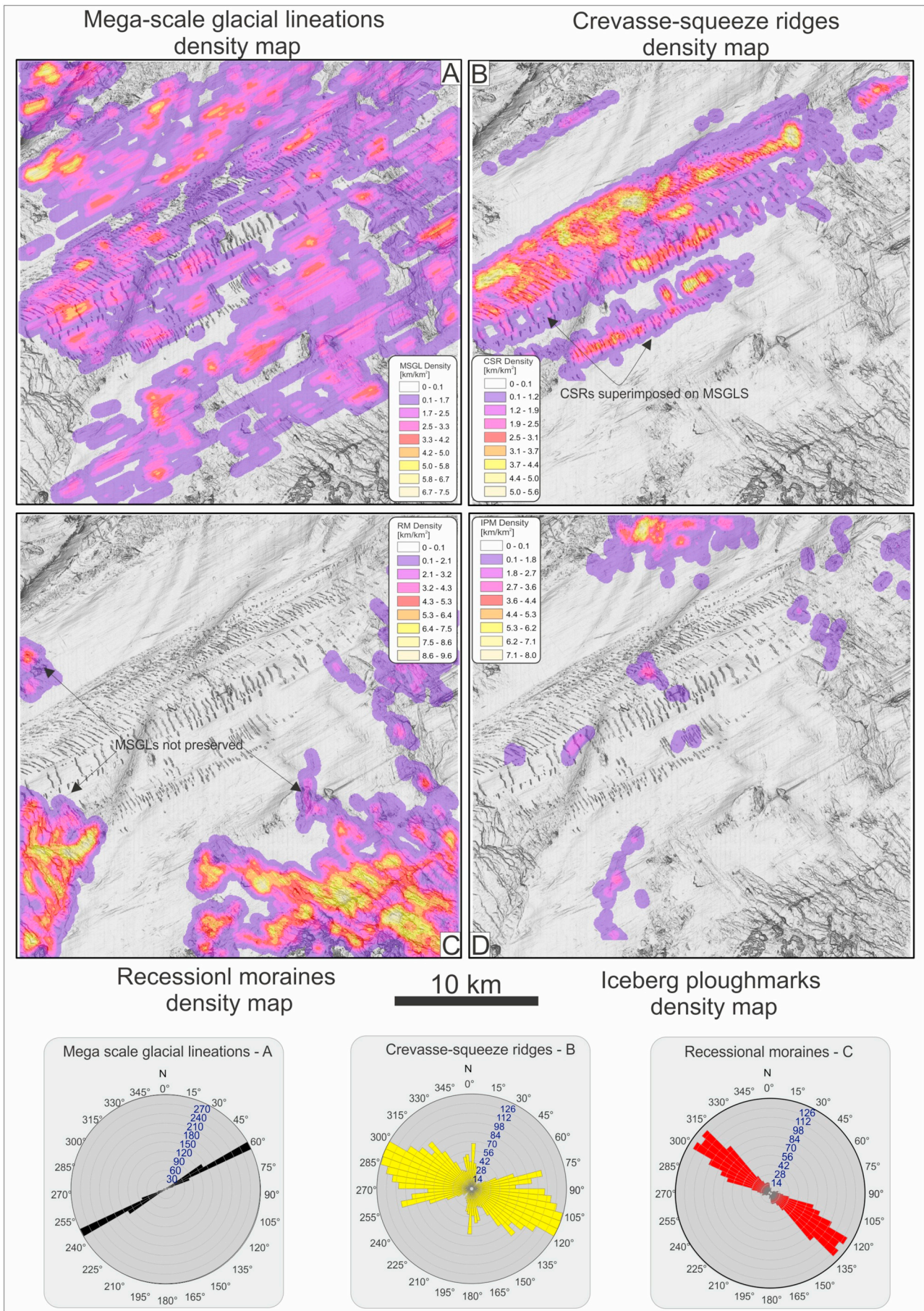
Recently, CSRs have been reported from the Bjørnøyrenna (Bear Island Trough) marine palaeo-ice stream in the Barents Sea (Andreassen et al., 2014a, 2014b; Bjarnadóttir et al., 2014). The CSRs described by Andreassen et al. (2014a, 2014b) and Bjarnadóttir et al. (2014) and the ones described in this study in Olgastretet have comparable metrics to those reported from terrestrial and marine terminating glaciers and terrestrial terminating ice streams (Evans et al., 2016; Evans and Rea, 1999). Crucially, their discovery indicates that CSRs can form under ice streams in marine settings and their preservation is consistent with shutdown followed by passive retreat. Lift-off of the ice stream due to marine drawdown and lowering of the ice surface profile may also be possible, but in such case the CSRs would not have been preserved. The sediments would have been lifted-off the seabed, incorporated into the ice stream and re-deposited as iceberg rafted debris.

At some time after shutdown, the ice stream was reactivated, as suggested by the presence of moraines upstream of the CSRs. The moraines found to the SE of the CSRs might also be linked to this reactivation.

The shutdown of an ice stream is relatively easier to understand in land terminating settings where the drawdown of ice mass by a surging ice stream reduces the driving stress of the ice, ultimately leading to its shutdown. In marine terminating ice streams, however, the velocity remains high all the way to the grounding line. Modern day Antarctic ice streams terminate in ice shelves which provide back-stress and buttressing, possibly facilitating a marine ice stream shutdown (De Angelis and Skvarca, 2003). We therefore propose that the presence of CSRs on marine palaeo-ice stream beds is consistent with the shutdown and passive retreat of an ice stream that terminated in an extensive ice shelf or thick ice melange.

4.2. Implications

The assemblage of landforms described in this paper comes from a different setting than the Bjørnøyrenna palaeo-ice stream bed used by Andreassen et al. (2014a, 2014b) to develop their marine ice stream retreat landsystem, and is used to further refine the landsystem model. In our dataset, no clear sediment apron/grounding line wedge (Batchelor and Dowdeswell, 2015; Dowdeswell and Fugelli, 2012; Powell and Alley, 1996; Simkins et al., 2018) can be observed, and large iceberg ploughmarks are absent from the area. CSRs in our study area are linear, comprising clearly segmented sections (Fig. 3B & C), similar to the stagnation ridges described by Bjarnadóttir et al. (2014) rather than the rhombohedral ridges described in the landsystem model by Andreassen et al. (2014a, 2014b). Finally, densely spaced curvilinear, festoon-like ridges (Fig. 3D & E), interpreted here as recessional moraines, were not found by Andreassen et al. (2014a, 2014b). These differences are interpreted to relate to the position of the two areas within a retreating marine ice stream landsystem (Fig. 3D & Fig. 7). The landform assemblage identified by Andreassen et al. (2014a, 2014b) is located within 5 km of the grounding line, identified by the grounding



(caption on next page)

Fig. 6. Landform density maps. A: Distribution of glacial lineations (MSGs). B: Distribution of CSRs over the study area. Note the co-occurrence of glacial lineations and CSRs superimposed on them. C: Distribution of ridges identified as recessional moraines in the study area. Note lack of glacial lineations underlying RMs. D: Distribution of iceberg ploughmarks over the study area. Higher density of ploughmarks is present only in the N part where the seabed is raised in comparison to the centre and S where RMs and CSRs are present. Rose diagrams show orientation of the long axes of linear landforms (MSGs, CSRs, RMs). Individual iceberg ploughmarks have no prevailing orientation and often curve around, therefore a rose diagram was not created.

zone wedge/sediment apron. The rhombohedral CSR network that they observe is therefore proximal to the grounding line and in a zone of increasing velocity and decreasing basal drag. No such sediment apron is present in the area investigated here and the CSRs have a linear rather than boxwork pattern. These resemble the CSRs described from the land terminating Maskwa ice stream, in the Laurentide ice sheet (Evans et al., 2016) which have been interpreted to have formed prior to ice stream shutdown, when the fast flowing trunk (an up-flow part) of the Maskwa ice stream was coming to a stop and fractures developed along shear zones between flow units moving at different velocities in an extensional stress regime (Fig. 7). We interpret the CSRs shown in Figs. 2 and 3 to be representative of a similar environment. Recessional moraines identified in the study area are located up flow and post-date formation of the CSRs. This implies that CSRs were preserved where the ice deglaciated passively, possibly by lift-off from the seabed following ice stream shutdown. Where recessional moraines are present, no CSRs or MSGs exist on the seabed. Recessional moraines in marine settings can only be formed when the ice margin is grounded on the seabed and is undergoing active retreat i.e. backstepping, punctuated by still stands/minor readvances, and with a continuous flux of ice and sediment to the grounding line. Such settings do not preserve CSRs on the seabed as they are reworked/destroyed (or never formed).

It is important to note that, in the Barents Sea, CSRs (linear stagnation ridges) have only previously been described from one other marine ice stream setting, in relatively deep water and further offshore (Bjarnadóttir et al., 2014). This may be due to a higher degree of reworking of the seabed by icebergs in shallower water or simply due to the lack of high resolution bathymetric data. CSRs have also been reported from other ice stream locations including the Gulf of Bothnia (Greenwood et al., 2017) and Antarctica (Greenwood et al., 2018; Klages et al., 2013, 2015).

The interpretation we present here can be summarised as follows. A period of ice streaming led to the formation of MSGs on the seafloor of Olgastretet, and the development of basal crevasses. This was followed by ice stream shutdown, generating the CSRs. At shutdown the ice stream terminated in an ice shelf, which remained intact as the grounding line retreated passively and/or lifted off the bed, protecting the MSG and CSRs from reworking by iceberg scouring as is often the case. Subsequently, the ice shelf/melange broke up removing the

backstress, ice velocities increased, leading to a readvance and/or initiation of active retreat and recessional moraine formation at the grounding line. As the grounding line retreated into shallower water only rarely were icebergs formed that had sufficient draft to scour the seabed. Together the presence of the ice shelf during deglaciation and, subsequent to its breakup, the retreat of the active margin into shallower water, explain the paucity of iceberg scours on the seabed.

4.3. Landsystem

Here we present an updated marine ice stream retreat landsystem model (Fig. 8) that utilises the reported observations, and revisited and revised data from Andreassen et al. (2014a, 2014b).

1. Ice margin position during ice stream shutdown is marked by a sediment apron (Fig. 8A) interpreted as a GZW (Andreassen et al., 2014b).
2. Large iceberg ploughmarks (Fig. 8A), can be found distally from the grounding zone (Andreassen et al., 2014b). They are usually located in front and/or on the surface of the GZW.
3. Rhombohedral, boxwork CSRs (Fig. 8B) found on the proximal side of the GZW develop during stagnation of the ice stream. They are limited to the ice marginal zone probably due to the highest fracture density in this area. They are always associated with, and superimposed, on MSGs (Andreassen et al., 2014b).
4. MSGs (Fig. 3A & Fig. 2) are found along the length of the ice stream and may continue onto the proximal side of the GZW (Andreassen et al., 2014b). Large-scale elongated sediment mounds reported by Andreassen et al. (2014a, 2014b), appear to be formed contemporaneously to the rhombohedral CSRs as both occur on the proximal, subglacial side of the sediment apron. They have a very distinctive morphology quite different from the MSGs reported from this and other papers as they are asymmetrical (widening down flow), wider (measured perpendicular to flow) and shorter (measured parallel to flow) (Bingham et al., 2017; Bjarnadóttir and Andreassen, 2016; Jamieson et al., 2016; Spagnolo et al., 2016). They resemble streamlined glacial lineations described by Ottesen et al. (2017) from marine terminating, surging glaciers in Svalbard, interpreted as a continuum of landforms ranging between MSGs and drumlins.
5. Linear CSRs (Fig. 3B & C, Fig. 4, Fig. 6, Fig. 8) develop further up ice from the rhombohedral CSRs, during ice streaming. They are related to shear zones between ice flow units within flow-parallel extensional stress regimes due to confining stress of the ice sheet beyond the ice stream margins (Evans et al., 2016), rather than radial extensional stress regime described from ice lobes resulting in more rhombohedral, fracture sets (Fig. 7).
6. Meltwater channels (Fig. 3H & Fig. 8B) develop subglacially, most likely during the ice stream shutdown when inefficient subglacial drainage changes to an efficient, channelized flow. The channels incise the MSGs, and therefore postdate ice streaming. The relative age of CSRs and channels is less clear, with examples of channels incising CSRs and other examples with little/no incision implying that they are contemporaneous to the formation of the channel. Most of the channels are located within the area covered by the CSRs.
7. Saw-tooth (Fig. 3D & E) and recessional moraines (Fig. 8C), indicate a phase of active ice margin retreat following passive retreat. The festoon shape of some of the ridges is probably due to the squeezing

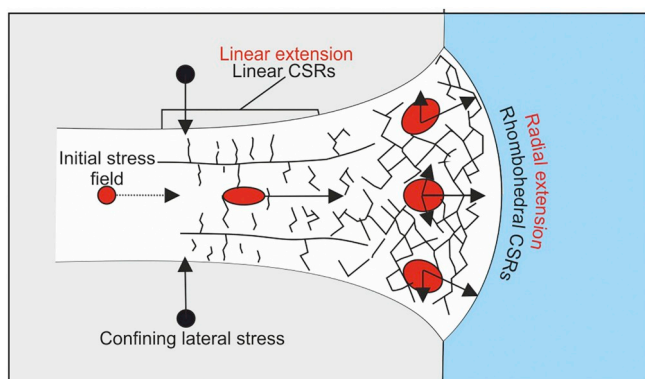


Fig. 7. Schematic interpretation of the formation of linear and rhombohedral CSRs as a function of stress field. In the area of primary linear extension the confining stress is provided by lateral margins of the ice stream. Radial extension is possible where the lateral confining stress is decreased towards the ice stream margin.

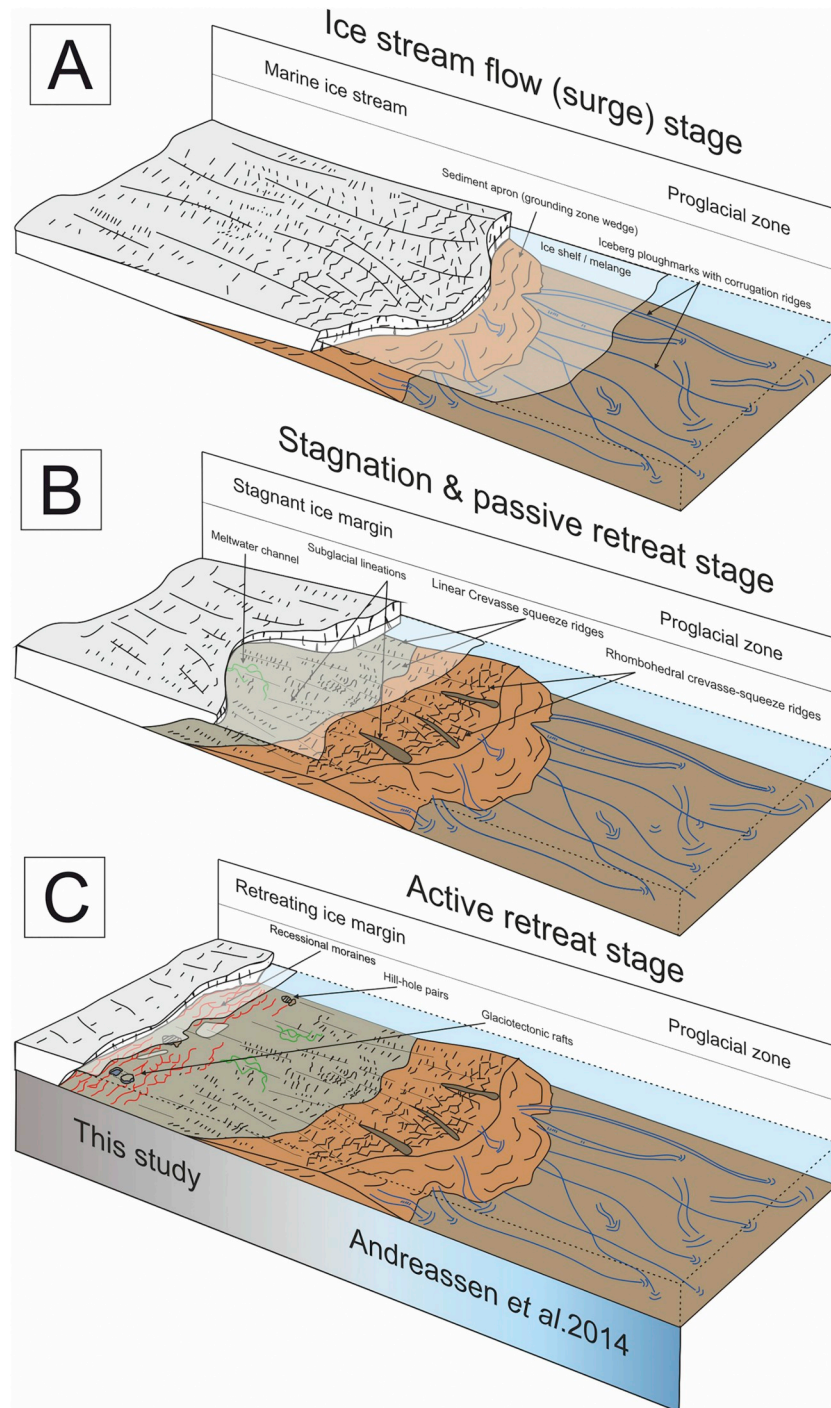


Fig. 8. Block diagram illustrating landform assemblage associated with marine ice stream shutdown. Landforms identified in proglacial and ice marginal zones after Andreassen et al. (2014a, 2014b). A: High velocity of ice streamflow (surge). Deposition of sedimentary apron by bulldozing and bottom-up hydrofracture development. B: Stagnation and lift-off of ice in the distal part. Sediments fill in basal fracture networks when ice decelerates. Passive retreat allows preservation of CSRs on the seabed. C: Active retreat at the grounding line resulting in destruction of CSRs and MSGSLs and deposition of recessional moraines.

of soft basal sediments into the remaining fracture network at the ice-bed interface during a periodic, possibly annual, ice re-advance.

8. Glacioteclonic bedforms (sediment rafts and hill-hole pairs) form when an ice stream is grounded and advancing and are preserved by the ice stream retreating. They most likely indicate basal freeze-on condition when less subglacial meltwater is delivered to the system. Some hill hole pairs may form during fast ice stream flow when there is a steep counterslope or discontinuity on the seabed oriented against the ice flow direction. They appear to be contemporary with the saw-tooth moraines.

9. During ice stream shutdown and subsequent stagnation, ice flow velocity decreased by several orders of magnitude, likely facilitated by the buffering effect of an ice shelf/melange. The ice stream then:

- Lifted off the seabed/retreated passively, allowing preservation of CSRs and MSGSLs.
- Subsequently, upstream of the CSRs and MSGSLs, the grounded ice stream margin began active retreating, depositing recessional moraines and destroying evidence of any underlying CSRs and MSGSLs.

Ice streaming, shutdown, passive retreat are reminiscent of

behaviour reported previously from surging glaciers (Evans et al., 2016; Evans and Rea, 1999; Ingólfsson et al., 2016), and can be accommodated by glacier physics and observed in numerical modelling (Alley et al., 2006; Bindschadler, 1997; Evans and Cofaigh, 2003; Feldmann and Levermann, 2017; Kristensen et al., 2007; Lelandais et al., 2018; Simon et al., 2014). To date, very limited morphological evidence for acceleration and stagnation (i.e. surging) of marine-based ice streams has been reported (Andreassen et al., 2014b). In documenting a second example of surge behaviour of a marine-based ice stream, we add support to the notion that such dynamics may be more commonly associated in these settings.

The interpretation that during ice sheet retreat, ice streams can switch on and off (in a surging manner), has major implications for both our understanding of palaeo and modern ice sheet dynamics. When modelling an ice sheet it is worth considering the “pulsating” rather than “steady flow” nature of an ice stream. The shutdown of a marine-based ice stream, may be facilitated by the buffering effect of an ice shelf and/or an ice melange with the opposite being true upon removal.

5. Conclusions

- We document a landform assemblage from the bed of a marine-based ice stream comprising MSGs, CSRs and recessional moraines. We interpret this to represent evidence for ice stream shutdown, followed by a phase of passive retreat and lift-off of the ice stream and finally re-establishment of active retreat of the ice margin farther up-flow.
- The land system model presented here builds on the model proposed by Andreassen et al. (2014a, 2014b) and provides the most complete description of the landform assemblage associated with marine ice streaming, shutdown, retreat and subsequent reactivation.
- Preservation of CSRs superimposed on MSGs formed under an ice stream is only possible following ice stream shutdown and passive retreat.
- Presence of linear CSRs in the study area indicates unidirectional extensional stress regime aligned with the ice stream flow direction most likely due to the lateral confining stress of the adjacent slow flowing ice and explains the absence of rhombohedral CSRs, in contrast to the marine-based ice stream land system described by Andreassen et al. (2014a, 2014b)
- Renewed active retreat is marked by recessional moraines up-flow from the CSR and MSG.
- Presence of an extensive ice shelf/ice melange, exerting a buffering effect on the ice stream is inferred and can play a role in marine ice stream shutdown.
- Lack of large scale iceberg ploughmarks in the study area indicates that the icebergs transiting through the area were smaller (shallower) than the contemporaneous water depth which is consistent with the passive deglaciation lift-off and ice shelf/melange hypothesis.
- Morphological evidence of marine ice stream shutdown characterised by surge-stagnation-reactivation cycles may be more common than previously thought.

Acknowledgements

The authors would like to thank NERC Oil and Gas CDT (<http://www.nerc-cdt-oil-and-gas.ac.uk>); NERC grant NE/M00578X/1 for the funding and support. We would also like to thank MAREANO (www.mareano.no) and EMODnet Bathymetry Consortium 2016 (<http://www.emodnet-bathymetry.eu>) for providing bathymetric data.

We would like to thank Sarah Greenwood and two anonymous reviewers whose comments helped us to improve the manuscript.

References

- Aber, J.S., Croot, D.G., Fenton, M.M., 1989. Hill-Hole Pair. Springer, Dordrecht, pp. 13–28. https://doi.org/10.1007/978-94-015-6841-8_2.
- Alley, R.B., Dupont, T.K., Parizek, B.R., Anandakrishnan, S., Lawson, D.E., Larson, G.J., Evenson, E.B., 2006. Outburst flooding and the initiation of ice-stream surges in response to climatic cooling: a hypothesis. *Geomorphology* 75, 76–89. <https://doi.org/10.1016/j.geomorph.2004.01.011>.
- Andreassen, K., Laberg, J.S., Vorren, T.O., 2008. Seafloor geomorphology of the SW Barents Sea and its glaci-dynamic implications. *Geomorphology* 97, 157–177.
- Andreassen, K., Winsborrow, M., 2009. Signature of ice streaming in Bjørnøyrenna, Polar North Atlantic, through the Pleistocene and implications for ice-stream dynamics. *Ann. Glaciol.* 50, 17–26.
- Andreassen, K., Bjarnadóttir, L.R., Dove, D., Dowdeswell, J.A., England, J.H., Funder, S., Hogan, K., Jennings, A., Krog Larsen, N., Kirchner, N., Landvik, J.Y., Mayer, L., Mikkelsen, N., Möller, P., Niessen, F., Nilsson, J., O'Regan, M., Polyak, L., Nørgaard-Pedersen, N., Stein, R., 2014a. Arctic Ocean glacial history. *Quat. Sci. Rev.* 92, 40–67. <https://doi.org/10.1016/j.quascirev.2013.07.033>.
- Andreassen, K., Winsborrow, M.C.M., Bjarnadóttir, L.R., Rüther, D.C., 2014b. Ice stream retreat dynamics inferred from an assemblage of landforms in the northern Barents Sea. *Quat. Sci. Rev.* 92, 246–257. <https://doi.org/10.1016/j.quascirev.2013.09.015>.
- Batchelor, C.L., Dowdeswell, J.A., 2014. The physiography of high arctic cross-shelf troughs. *Quat. Sci. Rev.* 92, 68–96. <https://doi.org/10.1016/j.quascirev.2013.05.025>.
- Batchelor, C.L., Dowdeswell, J.A., 2015. Ice-sheet grounding-zone wedges (GZWs) on high-latitude continental margins. *Mar. Geol.* 363, 65–92. <https://doi.org/10.1016/j.margeo.2015.02.001>.
- Bellwald, B., Planke, S., Polteau, S., Lebedeva-Ivanova, N., Hafeez, A., Faleide, J.I., Myklebust, R., 2018. Detailed Structure of Buried Glacial Landforms Revealed by High-resolution 3D Seismic Data in the SW Barents Sea. <https://doi.org/10.3997/2214-4609.201801161>.
- Benediktsson, Í.Ö., 2009. End Moraines and Ice-Marginal Processes of Surge-Type Glaciers.
- Benediktsson, N.Í.Ö., Ingólfsson, Ó., Schomacker, A., Kjaer, K.H., 2009. Formation of submarginal and proglacial end moraines: implications of ice-flow mechanism during the 1963–64 surge of Brúarjökull. *Iceland. Boreas* 38, 440–457. <https://doi.org/10.1111/j.1502-3885.2008.00077.x>.
- Bennett, M.R., 2003. Ice streams as the arteries of an ice sheet: their mechanics, stability and significance. *Earth-Science Rev.* 61, 309–339. [https://doi.org/10.1016/S0012-8252\(02\)00130-7](https://doi.org/10.1016/S0012-8252(02)00130-7).
- Bindschadler, R., 1997. Actively surging West Antarctic ice streams and their response characteristics. *Ann. Glaciol.* 24, 409–414. <https://doi.org/10.3189/S0260305500012520>.
- Bingham, R.G., Vaughan, D.G., King, E.C., Davies, D., Cornford, S.L., Smith, A.M., Arthern, R.J., Brisbourne, A.M., De Rydt, J., Graham, A.G.C., Spagnolo, M., Marsh, O.J., Shean, D.E., 2017. Diverse landscapes beneath Pine Island Glacier influence ice flow. *Nat. Commun.* 8, 1618. <https://doi.org/10.1038/s41467-017-01597-y>.
- Bjarnadóttir, L.R., 2016. Large subglacial meltwater features in the central Barents Sea. *Geology* 45, 1–45. <https://doi.org/10.1111/bor.12142>.
- Bjarnadóttir, L.R., Andreassen, K., 2016. Ice-stream landform assemblage in Kveithola, western Barents Sea margin. *Geol. Soc. London, Mem.* 46, 325–328. <https://doi.org/10.1144/m46.145>.
- Bjarnadóttir, L.R., Winsborrow, M.C.M., Andreassen, K., 2014. Deglaciation of the central Barents Sea. *Quat. Sci. Rev.* 92, 208–226.
- Boulton, G.S., van der Meer, J.J.M., Hart, J., Beets, D., Ruegg, G.H.J., Wateren, F.M., Jarvis, J., 1996. Till and moraine emplacement in a deforming bed surge - an example from a marine environment. *Quat. Sci. Rev.* 15, 961–987. [https://doi.org/10.1016/0277-3791\(95\)00091-7](https://doi.org/10.1016/0277-3791(95)00091-7).
- Christoffersen, P., Piotrowski, J.A., Nicolaj, K., Larsen, N.K., 2005. Basal processes beneath an Arctic glacier and their geomorphic imprint after a surge, Elisebreen, Svalbard. *Quat. Res.* 64, 125–137.
- Clark, C.D., 1993. Mega-scale glacial lineations and cross-cutting ice flow landforms. *Earth Surf. Process. Landf.* 18, 1–29.
- Clark, C.D., Stokes, C.R., 2001. Extent and basal characteristics of the M'Clintock Channel Ice Stream. *Quaternary International* 86 (1), 81–101. [https://doi.org/10.1016/S1040-6182\(01\)00052-0](https://doi.org/10.1016/S1040-6182(01)00052-0).
- Clarke, G.K.C., Collins, S.G., Thompson, D.E., 1984. Flow, thermal structure and sub-glacial conditions of a surge-type glacier. *Can. J. Earth Sci.* 21, 232–240.
- Clarke, G.K.C., 1987. Fast glacier flow: ice streams, surging, and tidewater glaciers. *J. Geophys. Res.* 92, 8835–8841. <https://doi.org/10.1029/JB092iB09p08835>.
- Cofaigh, C.O., Evans, D.J.A., Smith, I.R., 2010. Large-scale reorganization and sedimentation of terrestrial ice streams during late Wisconsinan Laurentide Ice Sheet deglaciation. *Geol. Soc. Am. Bull.* 122, 743–756. <https://doi.org/10.1130/B26476.1>.
- Consortium, Emod. B., 2016. Marine Information Service. EMODnet Digital Bathymetry (DTM). Marine Information Service <https://doi.org/10.12770/c7b53704-999d-4721-b1a3-04ec60c87238>.
- De Angelis, H., Skvarca, P., 2003. Glacier Surge after Ice Shelf Collapse. *Science* (80-.). vol. 299, pp. 1560–1562. <https://doi.org/10.1126/science.1077987>.
- Dowdeswell, J.A., Bamber, J.L., 2007. Keel depths of modern Antarctic icebergs and implications for sea-floor scouring in the geological record. *Mar. Geol.* 243, 120–131. <https://doi.org/10.1016/j.margeo.2007.04.008>.
- Dowdeswell, J.A., Fugelli, E.M.G., 2012. The seismic architecture and geometry of grounding-zone wedges formed at the marine margins of past ice sheets. *Bull. Geol. Soc. Am.* 124, 1750–1761. <https://doi.org/10.1130/B30628.1>.
- Dowdeswell, J.A., Hogan, K.A., Evans, J., Noormets, R., Ó Cofaigh, C., Ottesen, D., 2010.

- Past ice-sheet flow east of Svalbard inferred from streamlined subglacial landforms. *Geology* 38, 163–166. <https://doi.org/10.1130/G30621.1>.
- Dowdeswell, J.A., Canals, M., Jakobsson, M., Todd, B.J., Dowdeswell, E.K., Hogan, K.A., 2016. The variety and distribution of submarine glacial landforms and implications for ice-sheet reconstruction. *Geol. Soc. London, Mem.* 46, 519–552. <https://doi.org/10.1144/M46.183>.
- Elverhøi, A., Solheim, A., 1983. The Barents Sea ice sheet - a sedimentological discussion. *Polar Res.* 1, 23–42. <https://doi.org/10.1111/j.1751-8369.1983.tb00729.x>.
- Ely, J.C., Clark, C.D., Spagnolo, M., Stokes, C.R., Greenwood, S.L., Hughes, A.L.C., Dunlop, P., Hess, D., 2016. Do subglacial bedforms comprise a size and shape continuum? *Geomorphology* 257, 108–119. <https://doi.org/10.1016/j.geomorph.2016.01.001>.
- Enderlin, E.M., Howat, I.M., Jeong, S., Noh, M.-J., van Angelen, J.H., van den Broeke, M.R., 2014. An improved mass budget for the Greenland ice sheet. *Geophys. Res. Lett.* 41, 866–872. <https://doi.org/10.1002/2013GL059010>.
- Engelhardt, H., Kamb, B., 2013. Kamb Ice Stream flow history and surge potential. *Ann. Glaciol.* 54, 287–298. <https://doi.org/10.3189/2013AoG63A535>.
- Esteves, M., Bjarnadóttir, L.R., Winsborrow, M.C.M., Shackleton, C.S., Andreassen, K., 2017. Retreat patterns and dynamics of the Sentralbankrenna glacial system, Central Barents Sea. *Quat. Sci. Rev.* 169, 131–147. <https://doi.org/10.1016/J.QUASCIREV.2017.06.004>.
- Evans, D.J.A., Cofaigh, C.Ó., 2003. Depositional evidence for marginal oscillations of the Irish Sea ice stream in southeast Ireland during the last glaciation. *Boreas* 32, 76–101. <https://doi.org/10.1111/j.1502-3885.2003.tb01443.x>.
- Evans, D.J.A., Rea, B.R., 1999. Geomorphology and sedimentology of surging glaciers: a land-systems approach. *Ann. Glaciol.* 28, 75–82. <https://doi.org/10.3189/172756499781821823>.
- Evans, D.J.A., Lemmen, D.S., Rea, B.R., 1999. Glacial landforms of the southwest Laurentide ice sheet: Modern Icelandic analogues. *J. Quat. Sci.* 14 (7), 673–691. [https://doi.org/10.1002/\(SICI\)1099-1417\(199912\)14:7<673::AID-JQS467>3.0.CO;2-#](https://doi.org/10.1002/(SICI)1099-1417(199912)14:7<673::AID-JQS467>3.0.CO;2-#).
- Evans, D.J.A., Twigg, D.R., Rea, B.R., Orton, C., 2009. Surging glacier landform of tungnaárjökull, Iceland. *Journal of Maps* 5 (1), 134–151. <https://doi.org/10.4113/jom.2009.1064>.
- Evans, D.J.A., Storrar, R.D., Rea, B.R., 2016. Crevasse-squeeze ridge corridors: diagnostic features of late-stage palaeo-ice stream activity. *Geomorphology* 258, 40–50. <https://doi.org/10.1016/J.GEOMORPH.2016.01.017>.
- Feldmann, J., Levermann, A., 2017. From cyclic ice streaming to Heinrich-like events: the grow-and-surge instability in the Parallel Ice Sheet Model. *Cryosphere* 11, 1913–1932. <https://doi.org/10.5194/tc-11-1913-2017>.
- Flink, A.E., Noormets, R., Kirchner, N., Benn, D.I., Luckman, A., Lovell, H., 2015. The evolution of a submarine landform record following recent and multiple surges of Tunabreen glacier, Svalbard. *Quat. Sci. Rev.* 108, 37–50.
- Greenwood, S.L., Clason, C.C., Nyberg, J., Jakobsson, M., Holmlund, P., 2017. The Bothnian Sea ice stream: early Holocene retreat dynamics of the south-central Fennoscandian Ice Sheet. *Boreas* 46, 346–362. <https://doi.org/10.1111/bor.12217>.
- Greenwood, S.L., Simkins, L.M., Halberstadt, A.R.W., Prothro, L.O., Anderson, J.B., 2018. Holocene reconfiguration and readvance of the East Antarctic Ice Sheet. *Nat. Commun.* 9, 3176. <https://doi.org/10.1038/s41467-018-05625-3>.
- Hogan, K.A., Dowdeswell, J.A., Noormets, R., Evans, J., Ó Cofaigh, C., 2010. Evidence for full-glacial flow and retreat of the Late Weichselian Ice Sheet from the waters around Kong Karls Land, eastern Svalbard. *Quat. Sci. Rev.* 29, 3563–3582. <https://doi.org/10.1016/J.QUASCIREV.2010.05.026>.
- Hughes, A.L.C., Gyllencreutz, R., Lohne, Ø.S., Mangerud, J., Svendsen, J.I., Lohne, Øystein S., Mangerud, J., Svendsen, J.I., 2016. The last Eurasian ice sheets - a chronological database and time-slice reconstruction, DATED-1. *Boreas* 45, 1–45. <https://doi.org/10.1111/bor.12142>.
- Ingólfsson, Ó., Landvik, J.Y., 2013. The Svalbard–Barents Sea ice-sheet – Historical, current and future perspectives. *Quat. Sci. Rev.* 64, 33–60. <https://doi.org/10.1016/J.QUASCIREV.2012.11.034>.
- Ingólfsson, Ó., Benediktsson, Í.Ó., Schomacker, A., Kjær, K.H., Brynjólfsson, S., Jónsson, S.A., Korsgaard, N.J., Johnson, M.D., 2016. Glacial geological studies of surge-type glaciers in Iceland - Research status and future challenges. *Earth-Science Rev.* 152, 37–69. <https://doi.org/10.1016/j.earscirev.2015.11.008>.
- Jamieson, S.S.R., Stokes, C.R., Livingstone, S.J., Viel, A., Cofaigh, C., Hillenbrand, C.D., Spagnolo, M., 2016. Subglacial processes on an Antarctic ice stream bed. 2: can modelled ice dynamics explain the morphology of mega-scale glacial lineations? *J. Glaciol.* 62, 285–298. <https://doi.org/10.1017/jog.2016.19>.
- Johnson, P.G., 1975. Recent crevasse fillings at the terminus of the Donjek Glacier, St. Elias Mountains, Yukon Territory. *Quaestiones Geogr.* 2, 53–59.
- Joughin, I., Tulaczyk, S., Bindschadler, R., Price, S.F., 2002. Changes in west Antarctic ice stream velocities: observation and analysis. *J. Geophys. Res. Solid Earth* 107. <https://doi.org/10.1029/2001JB001029>. EPM 3-1-EPM 3-22.
- King, E.C., Hindmarsh, R.C.A., Stokes, C.R., 2009. Formation of mega-scale glacial lineations observed beneath a West Antarctic ice stream. *Nat. Geosci.* 2, 585–588.
- Klages, J.P., Kuhn, G., Hillenbrand, C.-D., Graham, A.G.C., Smith, J.A., Larter, R.D., Gohl, K., 2013. First geomorphological record and glacial history of an inter-ice stream ridge on the West Antarctic continental shelf. *Quat. Sci. Rev.* 61, 47–61. <https://doi.org/10.1016/J.QUASCIREV.2012.11.007>.
- Klages, J.P., Kuhn, G., Graham, A.G.C., Hillenbrand, C.-D., Smith, J.A., Nitsche, F.O., Larter, R.D., Gohl, K., 2015. Palaeo-ice stream pathways and retreat style in the easternmost Amundsen Sea Embayment, West Antarctica, revealed by combined multibeam bathymetric and seismic data. *Geomorphology* 245, 207–222. <https://doi.org/10.1016/J.GEOMORPH.2015.05.020>.
- Knies, J., Matthiessen, J., Vogt, C., Laberg, J.S., Hjelstuen, B.O., Smelror, M., Larsen, E., Andreassen, K., Eidvin, T., Vorren, T.O., 2009. The Plio-Pleistocene glaciation of the Barents Sea–Svalbard region: a new model based on revised chronostratigraphy. *Quat. Sci. Rev.* 28, 812–829. <https://doi.org/10.1016/J.QUASCIREV.2008.12.002>.
- Kristensen, T.B., Huuse, M., Piotrowski, J. a, Clausen, O.R., 2007. A morphometric analysis of tunnel valleys in the eastern North Sea based on 3D seismic data. *J. Quat. Sci.* 22, 801–815. <https://doi.org/10.1002/jqs>.
- Laberg, J.S., Vorren, T.O., 1996. The glacier-fed fan at the mouth of storfjorden trough, western barents sea: A comparative study. *Int. J. Earth Sci.* 85 (2), 338–349.
- Landvik, J.Y., et al., 1992. Weichselian stratigraphy and paleoenvironments at Bellsund, western Svalbard. *Boreas* 21, 335–358.
- Lelandais, T., Ravier, É., Pochat, S., Bourgeois, O., Clark, C., Mourgues, R., Strzeczynski, P., 2018. Modelled subglacial floods and tunnel valleys control the life cycle of transitory ice streams. *Cryosphere* 12, 2759–2772. <https://doi.org/10.5194/tc-12-2759-2018>.
- Matthews, J.A., Cornish, R., Shakesby, R.A., 1979. “Saw-Tooth” Moraines in Front of Bødalsbreen, Southern Norway. *J. Glaciol.* 22, 535–546. <https://doi.org/10.3189/S0022143000014519>.
- Newton, A.M.W., Huuse, M., 2017. Glacial geomorphology of the central Barents Sea: implications for the dynamic deglaciation of the Barents Sea Ice Sheet. *Mar. Geol.* 387, 114–131. <https://doi.org/10.1016/J.MARGE.2017.04.001>.
- Nielsen, T., Rasmussen, T.L., 2018. Reconstruction of ice sheet retreat after the Last Glacial maximum in Storfjorden, southern Svalbard. *Mar. Geol.* 402, 228–243. <https://doi.org/10.1016/J.MARGE.2017.12.003>.
- Ottesen, D., Dowdeswell, J.A., 2006. Assemblages of submarine landforms produced by tidewater glaciers in Svalbard. *J. Geophys. Res.* 111, F01016. <https://doi.org/10.1029/2005JF000330>.
- Ottesen, D., Dowdeswell, J.A., Benn, D.I., Kristensen, L., Christiansen, H.H., Christensen, O., Hansen, L., Lebesbye, E., Forwick, M., Vorren, T.O., 2008. Submarine landforms characteristic of glacier surges in two Spitsbergen fjords. *Quat. Sci. Rev.* 27 (15–16), 1583–1599. <https://doi.org/10.1016/j.quascirev.2008.05.007>.
- Ottesen, D., Dowdeswell, J.A., Bellec, V.K., Bjarnadóttir, L.R., 2017. The geomorphic imprint of glacier surges into open-marine waters: examples from eastern Svalbard. *Mar. Geol.* 392, 1–29. <https://doi.org/10.1016/J.MARGE.2017.08.007>.
- Patton, H., Andreassen, K., Bjarnadóttir, L.R., Dowdeswell, J.A., Winsborrow, M.C.M., Noormets, R., Polyak, L., Auriac, A., Hubbard, A., 2015. Geophysical constraints on the dynamics and retreat of the Barents Sea ice sheet as a paleobenchmark for models of marine ice sheet deglaciation. *Rev. Geophys.* 53, 1051–1098. <https://doi.org/10.1002/2015RG000495>.
- Patton, H., Hubbard, A., Andreassen, K., Winsborrow, M., Stroeven, A.P., 2016. The build-up, configuration, and dynamical sensitivity of the Eurasian ice-sheet complex to Late Weichselian climatic and oceanic forcing. *Quat. Sci. Rev.* 153, 97–121. <https://doi.org/10.1016/j.quascirev.2016.10.009>.
- Patton, H., Hubbard, A., Andreassen, K., Auriac, A., Whitehouse, P.L., Stroeven, A.P., Shackleton, C., Winsborrow, M., Heyman, J., Hall, A.M., 2017. Deglaciation of the Eurasian ice sheet complex. *Quat. Sci. Rev.* 169, 148–172. <https://doi.org/10.1016/J.QUASCIREV.2017.05.019>.
- Polyak, B., Scott, J., Lehman, V., Gataullin, A.J., Timothy, J., 1995. Two-step deglaciation of the southeastern Barents Sea. *Geology* 23 (6), 567–571. [https://doi.org/10.1130/0091-7613\(1995\)023<0567:TSDOTS>2.3.CO;2](https://doi.org/10.1130/0091-7613(1995)023<0567:TSDOTS>2.3.CO;2).
- Powell, R.D., Alley, R.B., 1996. Grounding-line systems: processes, glaciological inferences and the stratigraphic record. *Am. Geophys. Union* 169–187. <https://doi.org/10.1029/AR071p0169>.
- Rasmussen, T.L., Thomsen, E., Slubowska, M.A., Jessen, S., Solheim, A., Koç, N., 2007. Paleogeographic evolution of the SW Svalbard margin (76°N) since 20,000 ¹⁴C yr BP. *Quat. Res.* 67, 100–114.
- Rea, B.R., Evans, D.J.A., 2011. An assessment of surge-induced crevasse and the formation of crevasse squeeze ridges. *J. Geophys. Res.* 116 (F04005). <https://doi.org/10.1029/2011JF001970>.
- Rignot, E., Vaughan, D.G., Schmeltz, M., Dupont, T., MacAyeal, D., 2002. Acceleration of Pine Island and Thwaites Glaciers, West Antarctica. *Ann. Glaciol.* 34, 189–194. <https://doi.org/10.3189/172756402781817950>.
- Rise, L., Bellec, V.K., Ottesen, D., Bøe, R., Thorsnes, T., 2016. Hill–hole pairs on the Norwegian continental shelf. *Geol. Soc. London, Mem.* 46, 203–204. <https://doi.org/10.1144/M46.42>.
- Rüther, Denise Christina, Mattingdsal, Rune, Andreassen, Karin, Forwick, Matthias, Husum, Katrine, 2011. Seismic architecture and sedimentology of a major grounding zone system deposited by the Bjørnøyrenna Ice Stream during Late Weichselian deglaciation. *Quat. Sci. Rev.* (0277-3791) 30 (19–20), 2776–2792. <https://doi.org/10.1016/j.quascirev.2011.06.011>.
- Rüther, D.C., Andreassen, K., Spagnolo, M., 2013. Aligned glaciotectionic rafts on the central Barents Sea seafloor revealing extensive glaciotectionic erosion during the last deglaciation. *Geophys. Res. Lett.* 40, 6351–6355. <https://doi.org/10.1002/2013GL058413>.
- Rüther, D.C., Andreassen, K., Spagnolo, M., 2016. Aligned glaciotectionic rafts on the floor of the central Barents Sea. *Geol. Soc. Mem.* 46 (1), 189–190.
- Salvigsen, Otto, 1981. Radiocarbon Dated Raised Beaches in Kong Karls Land, Svalbard, and Their Consequences for the Glacial History of the Barents Sea Area. *Geografiska Annaler. Series A, Physical Geography* 63 (3/4), 283–291 (JSTOR, www.jstor.org/stable/520841).
- Sharp, Martin, 1985. Crevasse-Fill Ridges: A Landform Type Characteristic of Surging Glaciers. *Geografiska Annaler. Series A, Physical Geography* 67 (3/4), 213–220 (JSTOR, www.jstor.org/stable/521099).
- Siebert, M.J., Dowdeswell, J.A., 1996. Topographic control on the dynamics of the Svalbard-Barents Sea ice sheet. *Glob. Planet. Change* 12, 27–39. [https://doi.org/10.1016/0921-8181\(95\)00010-0](https://doi.org/10.1016/0921-8181(95)00010-0).
- Simkins, L.M., Greenwood, S.L., Anderson, J.B., 2018. Diagnosing ice sheet grounding line stability from landform morphology. *Cryosph.* 2707–2726. <https://doi.org/10.1002/2018JGLO00001>.

- 5194/tc-2018-44.
- Simon, Q., Hillarie-Marcel, C., St-Onge, G., Aandrews, J.T., 2014. North-eastern Laurentide, western Greenland and southern Innuitian ice stream dynamics during the last glacial cycle. *J. Quat. Sci.* 29, 14–26. <https://doi.org/10.1002/jqs.2648>.
- Solheim, A., Kristoffersen, Y., 1984. The physical environment, western barents sea. *Nor.Polarinst.Skr.* 179 B, 26.
- Spagnolo, M., Clark, C.D., Ely, J.C., Stokes, C.R., Anderson, J.B., Andreassen, K., Graham, A.G.C., King, E.C., 2014. Size, shape and spatial arrangement of mega-scale glacial lineations from a large and diverse dataset. *Earth Surf. Process. Landf.* 39 (11), 1432–1448.
- Spagnolo, M., Phillips, E., Piotrowski, J.A., Rea, B.R., Clark, C.D., Stokes, C.R., Carr, S.J., Ely, J.C., Ribolini, A., Wysota, W., Szuman, I., 2016. Ice stream motion facilitated by a shallow-deforming and accreting bed. *Nat. Commun.* 7, 10723. <https://doi.org/10.1038/ncomms10723>.
- Spagnolo, M., et al., 2017. The periodic topography of ice stream beds: Insights from the Fourier spectra of mega-scale glacial lineations. *J. Geophys. Res. Earth Surf.* 122, 1355–1373.
- Streuff, K., Forwick, M., Szczuciński, W., Andreassen, K., Ó Cofaigh, C., 2015. Submarine landform assemblages and sedimentary processes related to glacier surging in Kongsfjorden, Svalbard. *arktos* 1, 14. <https://doi.org/10.1007/s41063-015-0003-y>.
- Thomas, R., Scheuchl, B., Frederick, E., Harpold, R., Martin, C., Rignot, E., 2013. Continued slowing of the Ross Ice Shelf and thickening of West Antarctic ice streams. *J. Glaciol.* 59, 838–844. <https://doi.org/10.3189/2013JoG12J122>.
- Torbjørn Dahlgren, K.I., Vorren, T.O., Stoker, M.S., Nielsen, T., Nygård, A., Petter Sejrup, H., 2005. Late Cenozoic prograding wedges on the NW European continental margin: their formation and relationship to tectonics and climate. *Mar. Pet. Geol.* 22, 1089–1110. <https://doi.org/10.1016/J.MARPETGEO.2004.12.008>.
- Waller, R.I., Van Duk, T.A., Knudsen, Ó., 2008. Subglacial bedforms and conditions associated with the 1991 surge of Skeiðarárjökull, Iceland. *Boreas* 37, 179–194. <https://doi.org/10.1111/j.1502-3885.2007.00017.x>.
- Winsborrow, M.C.M., Andreassen, K., Corner, G.D., Laberg, J.S., 2010. Erratum to deglaciation of a marine-based ice sheet: Late weichselian palaeo-ice dynamics and retreat in the southern barents sea reconstructed from onshore and offshore glacial geomorphology [quat. sci. rev., 29, (2010), 424–442]. *Quat. Sci. Rev.* 29 (11–12), 1501. <https://doi.org/10.1016/j.quascirev.2010.03.009>.